Two-dimensional anisotropic N-vector models

Eytan Domany and Eberhard K. Riedel
Department of Physics, University of Washington, Seattle, Washington 98195
(Received 15 January 1979)

Two-dimensional anisotropic N-vector models are discussed in three contexts. (i) A comprehensive approach to the description of phase transitions in two-dimensional physical systems is outlined. It involves the identification of discrete models for critical phenomena in two-dimensional systems (such as adsorbed thin films) and their investigation by symmetry, duality, and Migdal renormalization-group methods. The identification is based on the Landau-Ginzburg-Wilson Hamiltonian concept and universality arguments. (ii) Relations among anisotropic continuous-spin Hamiltonians and discrete models are established by the Hubbard transformation and the Migdal renormalization-group transformation. Discrete models are conjectured to be equivalent to N-component continuous-spin models with local anisotropies. For example, it is shown that the Migdal recursion relations map the continuous-spin, cubic Heisenberg Hamiltonian onto the discrete cubic model. (iii) Many of the anisotropic N-vector Hamiltonians can be associated with discrete models that have the form of a generalized Potts model. Such a model, termed (N_α, N_β) model, is defined in terms of two interacting Potts-like variables associated with each lattice site, and is analyzed by duality and renormalization-group methods. The (N_α, N_β) Hamiltonian provides a unified description for large classes of discrete models. The concepts are exemplified by a detailed discussion of the two-dimensional Heisenberg model with cubic anisotropy, which has applications to the magnetic α-β phase transition in overlayers of molecular oxygen on graphite. New experiments for the study of this system are also discussed.

I. INTRODUCTION

In two-dimensions models possessing *continuous* symmetry (such as the classical XY and Heisenberg model) do not exhibit conventional long-range order at finite temperatures.[1] In contrast, models with *discrete* symmetry do undergo phase transitions into conventionally ordered phases. Obviously, a model has discrete symmetry when the underlying microscopic variable ("spin") is restricted to point into a finite number of allowed directions. Examples are Ising,[2] Potts,[3] Ashkin-Teller,[4] eight-vertex,[5] discrete cubic,[6,7] and discrete planar models.[8,9] Those Hamiltonians will be referred to as discrete models. When the basic variable is continuous (of fixed or varying length), the underlying symmetry of the model will be still discrete if the Hamiltonian includes local anisotropy fields. Examples are the classical XY and Heisenberg models with cubic anisotropy.[8,10] Those Hamiltonians will be referred to as anisotropic continuous-spin models. In the limit of infinite anisotropy, the appropriate discrete model is regained. A Landau symmetry analysis of discrete models[11] reveals also that they are related to anisotropic Landau-Ginzburg-Wilson (LGW) Hamiltonians of N-component order parameters.[12,13] In this sense, the whole set of models with discrete symmetry will be referred to as anisotropic N-vector models.[14]

The qualitatively different behaviors of models with continuous and discrete symmetries indicate that anisotropies play a very important role in two dimensions. Most theoretical studies have concentrated on the isotropic and extremely anisotropic limits. Continuous-spin models with finite anisotropy were only studied recently. Pelcovits and Nelson[10] considered the stability of isotropic N-vector spin systems against weak anisotropic perturbations in $D = 2 + \epsilon$ dimensions; José, Kadanoff, Kirkpatrick, and Nelson[8] studied the role of weak symmetry-breaking fields in the XY model in two dimensions. These studies indicate that the cubic anisotropy is relevant for Heisenberg and $N > 3$ models.[10] For the XY model the fourfold or "cubic" anisotropy is marginal, whereas the sixfold symmetry-breaking term is irrelevant.[8,15] In this paper, a renormalization-group argument for continuous-spin models with relevant symmetry-breaking terms is presented that applies also to the case of *finite* anisotropy. Since such perturbations iterate to larger values, the approach enables one to map a weakly anisotropic continuous-spin model onto a discrete spin model. In the limit of infinite anisotropy, the preferred directions of the continuous-spin

model become equivalent to the allowed directions of the discrete model. Here, Migdal's approximate renormalization-group method[16] is applied to the classical Heisenberg model with cubic anisotropy. The mapping constitutes the first step of a two-step renormalization-group approach to continuous-spin models.

Continuous-spin models are of great conceptual significance. On the basis of a universality hypothesis formulated by the authors,[17] one expects that the critical behavior of *two*-dimensional models and physical systems may be classified according to the appropriate LGW Hamiltonians. Effective LGW Hamiltonians can be constructed by Landau symmetry arguments[12,13] for physical systems and by the Hubbard transformation[18] for discrete models. The universality hypothesis is then used to relate the physical system and a discrete model. Various order-disorder transitions in adsorbed monolayers[19,20] and magnetic systems[17] give rise to LGW Hamiltonians that correspond to those of anisotropic N-vector models.

The second step of the renormalization-group procedure presented here concerns the treatment of discrete models. The first and crucial question is the choice of the "most appropriate" position space renormalization-group method.[16,21–23] In the present paper the method is identified by, first, observing that the model of interest (i.e., the discrete cubic model) is a special case of a more general one. For the general model, termed the (N_α, N_β) model, a number of exact results are derived by symmetry and duality arguments, which yield strong clues concerning the possible phase diagrams. Then, the appropriate renormalization-group method is selected by requiring that it preserve the symmetries of the model and yield as many of the exact results as possible. For the $(N_\alpha\, N_\beta)$ model, these conditions are best satisfied by the Migdal-Kadanoff approximate renormalization-group scheme.[16,23] We expect this method to yield quite reliable phase diagrams, but poor estimates for exponents.

The $(N_\alpha\, N_\beta)$ model is of considerable interest in its own right and, therefore, occupies a large part of this paper. It is defined as a system with two coupled, Potts-like variables ($\alpha=1,\ldots,N_\alpha$ and $\beta=1,\ldots,N_\beta$) associated with each site of a two-dimensional lattice. The model provides a unified description of a large variety of discrete models, including the Potts, Ashkin-Teller, planar and other anisotropic N-vector models. For example, the $N_\alpha=3$, $N_\beta=2$ model encompasses the planar six-state model, which has attracted attention recently.[8]

The approach is exemplified by a discussion of the two-dimensional Heisenberg model with cubic anisotropy. This model has applications[17] to the magnetic α-β phase transition in overlayers of molecular oxygen physisorbed on the basal plane of graphite. The latter system is being studied experimentally by neutron diffraction,[24] specific heat,[25] and magnetic susceptibility measurements.[26] Several other anisotropic N-vector models are realized experimentally.[17,19,20]

This paper is organized as follows. In Sec. II the continuous-spin cubic Heisenberg model is mapped onto the discrete cubic model by the Migdal transformation. In Sec. III the (N_α, N_β) model is introduced and discussed. Section IV deals with a symmetry analysis of special cases of the (N_α, N_β) model in terms of LGW Hamiltonians, obtained by the Hubbard transformation. The Migdal-Kadanoff recursion relations for the (N_α, N_β) model are derived in Sec. V. This section deals also with the phase diagrams for the cases $N_\alpha=N_\beta=2$ (Ashkin-Teller model) and $N_\alpha=3$, $N_\beta=2$ (six-state model) as obtained by the Migdal-Kadanoff method. The various concepts converge in Sec. VI, where a comprehensive approach to phase transitions in two-dimensional physical systems is outlined. The validity of the universality hypothesis is discussed and the methods are applied to the α-β transition in molecular oxygen on graphite. Finally, the work is summarized in Sec. VII.

II. MIGDAL RECURSION RELATIONS FOR CONTINUOUS-SPIN MODELS

In this section, we present the first step of our renormalization-group treatment of anisotropic continuous-spin models in two dimensions, using the Heisenberg model with cubic anisotropy as an example. Under the Migdal transformation, it maps onto the discrete cubic model.

We start from the Hamiltonian for continuous spins of fixed length $|\vec{S}_i|^2=1$, on a square lattice,

$$\frac{\mathcal{H}}{k_B T}=-K\sum_{\langle i,j\rangle}\vec{S}_i\cdot\vec{S}_j-v\sum_i\sum_{\alpha=1}^{3}(S_i^\alpha)^4\ . \tag{2.1}$$

The first term represents the nearest-neighbor isotropic exchange interaction and the second one the local anisotropy field of cubic symmetry. For $v>0$ the spins point preferredly along the six (1,0,0) directions, and for $v<0$ along the eight (1,1,1) directions.

The model (2.1) is investigated here by Migdal's approximate renormalization-group method.[16] First, the Hamiltonian is expressed as a sum over contributions associated with bonds

$$\begin{aligned}\frac{\mathcal{H}}{k_B T}&=-\sum_{\langle i,j\rangle}U^{(0)}(\vec{S}_i,\vec{S}_j)\ ,\\ U^{(0)}(\vec{S}_i,\vec{S}_j)&=K\,\vec{S}_i\cdot\vec{S}_j\\ &\quad+\tfrac{1}{4}v\sum_\alpha[(S_i^\alpha)^4+(S_j^\alpha)^4]\ .\end{aligned} \tag{2.2}$$

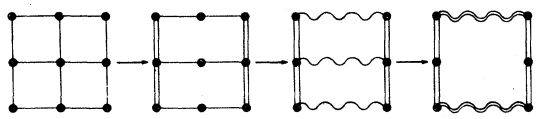

FIG. 1. Schematic representation of the Migdal renormalization-group procedure for $\lambda=2$. The new interactions are represented by double wavy lines.

The "splitting" of the single-site anisotropy term has been used previously.[8,27] Second, the renormalization-group procedure is realized as indicated in Fig. 1. Every other vertical bond (i.e., $U^{(0)}$) is shifted and the traces over spins connected to only two (horizontal) neighbors are performed. Then every other horizontal bond is shifted, which yields the new coupling, $U^{(1)}$. Upon iteration, this procedure generates a recursion relation of the form

$$\exp[U^{(n+1)}(\vec{S}_1,\vec{S}_2)]=\left[\int d\vec{S}\exp[U^{(n)}(\vec{S}_1,\vec{S})+U^{(n)}(\vec{S},\vec{S}_2)]\right]^2 . \tag{2.3}$$

The integration is over the surface of a unit sphere.

We performed the integration in Eq. (2.3) numerically and at each stage of the iteration characterized $U^{(n)}$ by its projection onto the first few functions of an orthonormal set. The functions $U^{(n)}$ were evaluated on a discrete set of points. For a function of a *single* spin that possesses cubic symmetry, the unit sphere can be divided into 48 equivalent triangles. Allowing n points in each triangle, a function of *two* spin variables, $\vec{S}_1$ and $\vec{S}_2$, has to be evaluated at $48n^2$ points; i.e., the same number of integrals has to be determined for each iteration. To keep the computation manageable we did not work with a very dense mesh (high n). For $n=10$ our integration routine had about 1% accuracy. Thus, for this value of n the recursion relations can be used as a qualitative tool to study the renormalization-group flows and to obtain the global phase diagrams. The functions used to characterize the coupling $U^{(n)}(\vec{S}_1,\vec{S}_2)$ are given by

$$\begin{aligned}
&\phi_0=C_0 ,\\
&\phi_1=C_1\vec{S}_1\cdot\vec{S}_2 ,\\
&\phi_2=C_2[3\sum_\alpha (S_1^\alpha)^2(S_2^\alpha)^2-1] ,\\
&\phi_3=C_3(S_1^xS_1^yS_2^xS_2^y+S_1^yS_1^zS_2^yS_2^z+S_1^zS_1^xS_2^zS_2^x) ,\\
&\phi_4=C_4\left[\sum_\alpha[(S_1^\alpha)^4+(S_2^\alpha)^4]-2.4\right] .
\end{aligned} \tag{2.4}$$

The constants C_i ensure orthonormality, i.e.,

$$\int d\vec{S}_1\,d\vec{S}_2\phi_i(\vec{S}_1\vec{S}_2)\phi_j(\vec{S}_1\vec{S}_2)=\delta_{i,j} . \tag{2.5}$$

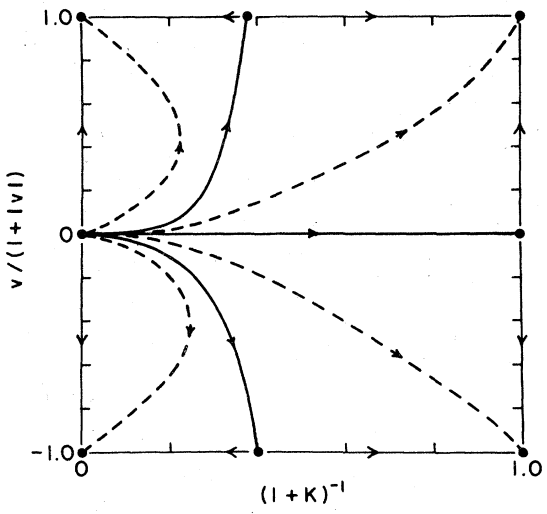

FIG. 2. Flow diagram for the two-dimensional Heisenberg model with cubic anisotropy, as obtained by the Migdal recursion scheme, Eq. (2.3).

After each iteration, the expansion coefficients

$$A_i^{(n)}=\int d\vec{S}_1\,d\vec{S}_2U^{(n)}(\vec{S}_1,\vec{S}_2)\phi_i(\vec{S}_1,\vec{S}_2) \tag{2.6}$$

were evaluated. Of these, $A_0^{(n)}$ represents a constant, $A_1^{(n)}$ was identified as $K\sim T^{-1}$, and the on-site anisotropy parameter v is proportional to A_4.

The projections of the renormalization-group trajectories onto the $((1+K)^{-1}, v/(1+|v|))$ plane are shown schematically in Fig. 2, for both $v^{(0)}>0$ and $v^{(0)}<0$. The isotropic Heisenberg model ($v^{(0)}=0$) does not exhibit a phase transition in two dimensions.[16,28] Only two fixed points exist on the $v=0$ line, an unstable one at zero temperature and a stable one at infinite temperature. When the initial anisotropy is nonzero, the recursion relations take the model (2.1) to the extremely anisotropic limit as discussed in Sec. I. In this limit the spins can point *only* into the preferred directions determined by the anisotropy term. A separatrix between high- and low-temperature behavior does exist and the critical behavior is controlled by a fixed point at infinite anisotropy, i.e., that of a discrete spin Hamiltonian.

Once the appropriate discrete model is identified, the first stage of the procedure is complete. For further investigations of the critical behavior and phase diagram we will use the discrete model as a starting point.

One notes, that although the initial nearest-neighbor interaction is isotropic, $\vec{S}_i\cdot\vec{S}_j$, the recursion relations generate a more general one through the functions $\phi_2,\phi_3,\ldots$. Therefore, the Migdal renormalization-group procedure maps the continuous-spin cubic Heisenberg Hamiltonian onto a discrete cubic model exhibiting the most general in-

teraction consistent with cubic symmetry. For example, for the case $v > 0$ the interaction between two nearest neighbors depends on two parameters. The relative angle between two neighboring spins can assume the values 0, 90°, 180°, and the two parameters that define the discrete model are the energy differences $E(90) - E(0)$, and $E(180) - E(0)$. This general discrete cubic model was investigated by Kim, Levy, and Uffer[6] and Aharony.[7] It can be described by placing at each site of a square lattice a three-state Potts and an Ising variable, $\alpha = 1, 2, 3$ and $\beta = 1, 2$, respectively. The most general nearest-neighbor interaction consistent with cubic symmetry is

$$-K_{0,0}\delta_{\alpha_1,\alpha_2}\delta_{\beta_1,\beta_2} - K_{0,1}\delta_{\alpha_1,\alpha_2}(1-\delta_{\beta_1,\beta_2}) - K'(1-\delta_{\alpha_1,\alpha_2}) \quad . \tag{2.7}$$

In terms of angles between neighboring spins the correspondence is

$$E(0) = -K_{0,0}, \quad E(180) = -K_{0,1}, \quad E(90) = -K' \quad .$$

A more general discrete model that encompasses the cubic one is discussed in the next sections.

III. THE (N_α, N_β) MODEL

In this section, we define the (N_α, N_β) model, discuss it by symmetry and duality arguments, and list special cases.

A. Definition

The (N_α, N_β) model is a generalization of the Potts model.[3] Consider a square lattice (or for general D a hypercubic lattice) and associate with each lattice site *two* discrete variables that assume N_α and N_β values, respectively,

$$\alpha_i = 1, \ldots, N_\alpha; \quad \beta_i = 1, \ldots, N_\beta \quad . \tag{3.1}$$

Then the (N_α, N_β) model is defined by the Hamiltonian

$$\begin{aligned}\frac{\mathcal{H}}{k_B T} = -\sum_{\langle i,j\rangle} [&K_{0,0}\delta_{\alpha_i,\alpha_j}\delta_{\beta_i,\beta_j} \\ &+ K_{1,0}(1-\delta_{\alpha_i,\alpha_j})\delta_{\beta_i,\beta_j} \\ &+ K_{0,1}\delta_{\alpha_i,\alpha_j}(1-\delta_{\beta_i,\beta_j}) \\ &+ K_{1,1}(1-\delta_{\alpha_i,\alpha_j})(1-\delta_{\beta_i,\beta_j})] \quad .\end{aligned} \tag{3.2}$$

The Hamiltonian is invariant under the direct product of the permutations of the α and β indices. Each nearest-neighbor pair $\langle i,j\rangle$ is associated with four possible energies. If the variables α_i, β_i at one site, i, are fixed, the $N_\alpha N_\beta$ states at a nearest-neighbor site, j, divide into four classes characterized by the energies $K_{0,0}$, $K_{1,0}$, $K_{0,1}$, and $K_{1,1}$ with the respective multiplicities 1, $N_\alpha - 1$, $N_\beta - 1$, and $(N_\alpha - 1)(N_\beta - 1)$. Hence the thermodynamic properties of the model can be described in terms of the values of three parameters. A convenient choice is

$$x_\alpha = \exp(K_{1,0} - K_{0,0}); \quad x_\beta = \exp(K_{0,1} - K_{0,0}) \quad ;$$
$$z = \exp(K_{1,1} - K_{0,0}) \quad . \tag{3.3}$$

In the case of a ferromagnetic ground state (i.e., $K_{0,0} \geq K_{1,0}, K_{0,1}, K_{1,1}$) the physical parameter space is in the cube $0 \leq x_\alpha, x_\beta, z \leq 1$.

Systems described by the Hamiltonian (3.2) exhibit a rich variety of critical behavior. The models contained in Eq. (3.2), their geometrical interpretations and symmetries will be discussed in detail in Secs. III C and IV. Some results for the general (N_α, N_β) model are summarized below.

By rewriting the Hamiltonian (3.2) in the form

$$\frac{\mathcal{H}}{k_B T} = -\sum_{\langle i,j\rangle} [(K_{0,0} - K_{1,0} - K_{0,1} + K_{1,1})\delta_{\alpha_i,\alpha_j}\delta_{\beta_i,\beta_j} + (K_{0,1} - K_{1,1})\delta_{\alpha_i,\alpha_j} + (K_{1,0} - K_{1,1})\delta_{\beta_i,\beta_j} + K_{1,1}] \quad , \tag{3.4}$$

one sees that it reduces to two decoupled Potts models (of N_α and N_β components) when

$$x_\alpha x_\beta = z \quad , \tag{3.5}$$

i.e., $K_{0,0} - K_{1,0} - K_{0,1} + K_{1,1} = 0$, and to a $N_\alpha N_\beta$-state Potts model when

$$x_\alpha = x_\beta = z \quad , \tag{3.6}$$

i.e., $K_{1,0} = K_{0,1} = K_{1,1}$. The "decoupled" surface (3.5) and line of special symmetry (3.6) are shown in

Fig. 3. The special points $x_\alpha = x_\beta = z = 0$ and $x_\alpha = x_\beta = z = 1$ describe the general model at the temperatures $T = 0$ and $T = \infty$. The points $x_\alpha = 1$, $x_\beta = z = 0$ and $x_\alpha = z = 0$, $x_\beta = 1$ correspond to the situation of one system at $T = 0$ and the other at $T = \infty$.

The phases that exist on the decoupled surface are exhibited in Fig. 4, which shows the projection of that surface onto the $z = 0$ plane. The intersection of the decoupled surface (3.5) with the plane

$$x_\alpha = [1 + (N_\alpha)^{1/2}]^{-1}$$

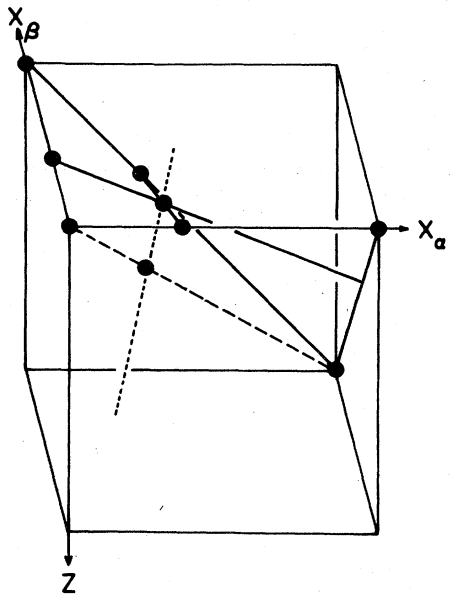

FIG. 3. Physical parameter space for the (N_α, N_β) model of Eq. (3.2), $0 \leq x_\alpha, x_\beta, z \leq 1$. On the surface $x_\alpha x_\beta = z$ (solid lines) the model describes two decoupled Potts models with N_α and N_β components, and on the line $x_\alpha = x_\beta = z$ (dashed line) a $N_\alpha N_\beta$-component Potts model. All points on the dotted line are self-dual. The heavy dots represent fixed points of a renormalization-group calculation discussed in Sec. V C.

defines a line of phase transitions of N_α-state Potts type. A similar relation defines a N_β Potts transition line. These two lines meet at the special decoupled multicritical point

$$x_\alpha = [1 + (N_\alpha)^{1/2}]^{-1}; \quad x_\beta = [1 + (N_\beta)^{1/2}]^{-1} \; ;$$
$$z = x_\alpha x_\beta \tag{3.7}$$

at which both types of behavior occur. On the line (3.6), the $N_\alpha N_\beta$-state Potts model exhibits a phase transition at

$$z = [1 + (N_\alpha N_\beta)^{1/2}]^{-1} \; . \tag{3.8}$$

Note that the transition of the Potts model in two dimensions is second order when $N \leq 4$ and first order when $N > 4$.[29] In three dimensions first-order transitions are expected for $N \geq 3$.[30]

B. Duality transformation

Wu and Wang[31] have given a formulation of the duality transformation for two-dimensional spin models that can be easily applied to the (N_α, N_β) model. The partition function for the (N_α, N_β) model is

$$Z = \sum_{\{\alpha,\beta\}} \prod_{\langle i,j \rangle} U_{\alpha_i \beta_i, \alpha_j \beta_j} \; , \tag{3.9}$$

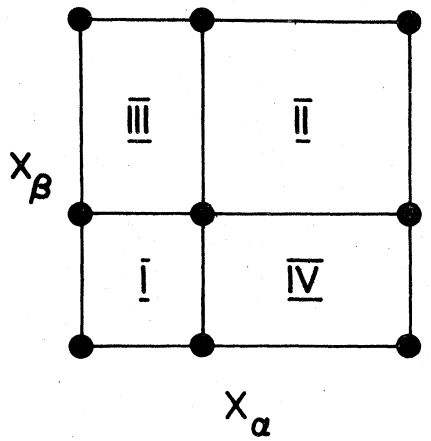

FIG. 4. Projection of the "decoupled" surface, $x_\alpha x_\beta = z$, of Fig. 3 onto the $z = 0$ plane. There are four phases: completely ordered (I), complete disordered (II), β disordered and α ordered (III) and vice versa (IV).

with

$$U_{\alpha_i \beta_i, \alpha_j \beta_j} = \exp\left[K(\alpha_i, \beta_i; \alpha_j, \beta_j)\right] \; . \tag{3.10}$$

Consider first the case $N_\beta = 1$. The matrix U reduces to a $N_\alpha \times N_\alpha$ matrix, $U_{\alpha\alpha'} = \exp[K(\alpha, \alpha')]$. The matrix is cyclic,

$$U_{\alpha\alpha'} = u(\bar{\alpha}), \quad \bar{\alpha} = \alpha - \alpha' (\mathrm{mod} N_\alpha) \; , \tag{3.11}$$

and has the eigenvalues

$$\lambda(\eta) = \sum_{\alpha=1}^{N_\alpha} u(\alpha) \exp\left[\frac{-2\pi i \eta \alpha}{N_\alpha}\right] \tag{3.12}$$

and eigenvectors

$$v_\alpha^{(\eta)} = N_\alpha^{-1/2} \exp\left[\frac{2\pi i \eta \alpha}{N_\alpha}\right] \; , \tag{3.13}$$

where the index $\eta = 0, \ldots, N_\alpha - 1$. The results (3.12) and (3.13) hold for arbitrary cyclic matrices, i.e., interactions satisfying $K(\alpha_i, \alpha_j) = K(\alpha_{ij})$ with $\alpha_{ij} = \alpha_i - \alpha_j \pmod{N_\alpha}$. Wu and Wang[31] have shown that the partition function of a system with couplings $u(\alpha)$ on the lattice L is equal (up to multiplicative constants) to that of a system defined on the lattice L^D, which is dual to L, with couplings $\lambda(\eta)$. Hence Eq. (3.12) defines a duality transformation.

Consider now the case of general N_α and N_β. The matrix (3.10) can be expressed by a $N_\beta \times N_\beta$ matrix of $N_\alpha \times N_\alpha$ matrices,

$$U_{\alpha\beta, \alpha'\beta'} = U_{\alpha,\alpha'}^{(\beta,\beta')} \; , \tag{3.14}$$

which are defined by

$$U_{\alpha,\alpha'}^{(\beta,\beta')} = U_{\alpha,\alpha'}^{(0)} \delta_{\beta,\beta'} + U_{\alpha,\alpha'}^{(1)} (1 - \delta_{\beta,\beta'}) \tag{3.15a}$$

and

$$U^{(0)}_{\alpha,\alpha'} = e^{K_{0,0}}\delta_{\alpha,\alpha'} + e^{K_{1,0}}(1-\delta_{\alpha,\alpha'}) \ ,$$
$$U^{(1)}_{\alpha,\alpha'} = e^{K_{0,1}}\delta_{\alpha,\alpha'} + e^{K_{1,1}}(1-\delta_{\alpha,\alpha'}) \ . \tag{3.15b}$$

This matrix is block cyclic. Hence the eigenvectors can be written as direct products of eigenvectors (3.13),

$$v^{(\eta,\zeta)}_{\alpha,\beta} = v^{(\eta)}_{\alpha}\, v^{(\zeta)}_{\beta} \tag{3.16}$$

with $\eta = 0,\ldots,N_\alpha - 1$ and $\zeta = 0,\ldots,N_\beta - 1$. There are four distinct eigenvalues, $\lambda_{\eta,\zeta}$, that correspond to eigenvectors with $\eta = \zeta = 0$; $\eta \neq 0$, $\zeta = 0$; $\eta = 0$, $\zeta \neq 0$; and $\eta \neq 0$, $\zeta \neq 0$,

$$\begin{aligned}
\lambda_{0,0} &= e^{\tilde{K}_{0,0}} = e^{K_{0,0}} + (N_\alpha - 1)e^{K_{1,0}} + (N_\beta - 1)e^{K_{0,1}} + (N_\alpha - 1)(N_\beta - 1)e^{K_{1,1}} \ , \\
\lambda_{1,0} &= e^{\tilde{K}_{1,0}} = e^{K_{0,0}} - e^{K_{1,0}} + (N_\beta - 1)(e^{K_{0,1}} - e^{K_{1,1}}) \ , \\
\lambda_{0,1} &= e^{\tilde{K}_{0,1}} = e^{K_{0,0}} - e^{K_{0,1}} + (N_\alpha - 1)(e^{K_{1,0}} - e^{K_{1,1}}) \ , \\
\lambda_{1,1} &= e^{\tilde{K}_{1,1}} = e^{K_{0,0}} - e^{K_{1,0}} - e^{K_{0,1}} + e^{K_{1,1}} \ .
\end{aligned} \tag{3.17}$$

This transformation maps the (N_α, N_β) model (3.2) onto a similar model, in which the couplings $K_{l,m}$ are replaced by the dual couplings $\tilde{K}_{l,m}$. For $N_\beta = 1$ the equations reduce to the duality transformation for the N_α-state Potts model. In terms of the variables x_α, x_β, z of Eq. (3.3) the duality transformation reads

$$\begin{aligned}
\tilde{x}_\alpha &= [1 - x_\alpha + (N_\beta - 1)(x_\beta - z)]/\Delta \ , \\
\tilde{x}_\beta &= [1 - x_\beta + (N_\alpha - 1)(x_\alpha - z)]/\Delta \ , \\
\tilde{z} &= (1 - x_\alpha - x_\beta + z)/\Delta \ , \\
\Delta &= 1 + (N_\alpha - 1)x_\alpha + (N_\beta - 1)x_\beta + (N_\alpha - 1)(N_\beta - 1)z \ .
\end{aligned} \tag{3.18}$$

Defining $\vec{x} = (x_\alpha, x_\beta, z)$, we shall use the notation

$$\vec{\tilde{x}} = \vec{D}(\vec{x}) \tag{3.19}$$

for this mapping.

We list several properties of the transformation. It is self-inverse, i.e., $\vec{D}[\vec{D}(\vec{x})] = \vec{x}$. The zero-temperature point maps onto $T = \infty$, and vice versa. When $\vec{x}$ is on the decoupled surface of Eq. (3.5), so is $\vec{\tilde{x}}$. In this case the transformations for the variables x_α and x_β decouple; each satisfies an equation of the form ($\gamma = \alpha$ or β)

$$\tilde{x}_\gamma = (1 - x_\gamma)/[1 + (N_\gamma - 1)x_\gamma] \ , \tag{3.20}$$

and $\tilde{z} = \tilde{x}_\alpha \tilde{x}_\beta$. Thus in Fig. 4, the transformation maps region I onto II, III onto IV, and vice versa. The multicritical point maps onto itself. The $N_\alpha N_\beta$ Potts symmetry (e.g., $x_\alpha = x_\beta = z$) is also preserved by $\vec{D}$; in this case the Eq. (3.19) reduce to

$$\tilde{x} = (1 - x)/[1 + (N_\alpha N_\beta - 1)x] \ , \tag{3.21}$$

and the $N_\alpha N_\beta$-component transition point is self-dual.

The plane defined by [see Eq. (3.18)]

$$\Delta(x_\alpha, x_\beta, z) = (N_\alpha N_\beta)^{1/2} \tag{3.22}$$

maps onto itself. The transformation has a set of fixed points, i.e., $\vec{D}(\vec{x}) = \vec{x}$; these points lie on the straight line defined by the intersection of the planes (3.22) and

$$x_\alpha + x_\beta + [(N_\alpha N_\beta)^{1/2} - 1]z = 1 \ . \tag{3.23}$$

This straight line passes through the decoupled multicritical point and the $N_\alpha N_\beta$-component Potts transition point, and is also shown in Fig. 3. For $N_\alpha \neq N_\beta$, the model exhibits a phase transition at all points of the self-dual line. This is not the case for $N_\alpha = N_\beta = 2$.[32]

C. Special cases and geometric interpretations

The (N_α, N_β) model (3.2) encompasses a large number of discrete models for special choices of N_α and N_β. The kinds of transitions that these models exhibit depend on the relative magnitude of the coupling constants (3.3).

a. *Potts Models.* In the limit of general N_α and $N_\beta = 1$, the model (3.2) equals the N_α-component Potts model.[3] The nearest-neighbor energies split into two classes with 1 and $N_\alpha - 1$ states of energy, $K_{0,0}$ and $K_{1,0}$, respectively. A geometrical interpretation in terms of a set of N_α vectors with $N_\alpha - 1$ components has been given by Zia and Wallace.[33] The general (N_α, N_β) model exhibits transitions of the Potts type on various planes (lines) in the (x_α, x_β, z) space as discussed in Sec. III A.

b. *Cubic models.* For general N_α and $N_\beta = 2$ *and* $x_\alpha = z$, the (N_α, N_β) model specializes to the discrete cubic model[6,7]

$$\frac{\mathcal{H}}{k_B T} = -\sum_{\langle i,j \rangle} (K_1 \sigma_i \sigma_j \delta_{\alpha_i,\alpha_j} + K_2 \delta_{\alpha_i,\alpha_j}) \ , \tag{3.24}$$

Here the identity $\delta_{\beta_i,\beta_j} = \frac{1}{2}(1 + \sigma_i \sigma_j)$ has been used,

where $\sigma_i = \pm 1$. The nearest-neighbor interaction energies separate into three classes with 1, $2(N_\alpha - 1)$, 1 states of energy K_{00}, $K_{10} = K_{11}$, and K_{01}, respectively. A spin representation of Eq. (3.24) in terms of the N_α-component vectors $(\pm 1, 0, \ldots, 0)$; ...; $(0, \ldots, 0, \pm 1)$ is possible. The duality transformation (3.18) maps the plane $x_\alpha = z$ onto $\tilde{x}_\beta = \tilde{z}$ (and, similarly, $x_\beta = z$ onto $\tilde{x}_\alpha = \tilde{z}$). On the plane $x_\beta = z$, the nearest-neighbor energies separate into three classes with 1, $N_\alpha - 1$, N_α states of energy $K_{0,0}$, $K_{1,0}$, $K_{0,1} = K_{1,1}$, respectively. A vector-spin representation of this $2N_\alpha$-state model requires a set of $2(N_\alpha - 1)$-component vectors. Although the symmetries of the models on the $x_\alpha = z$ and $x_\beta = z$ planes are different they are expected to exhibit the same kinds of phase transitions since they are related by duality.

c. *Ashkin-Teller model.* With $N_\alpha = N_\beta = 2$ and $\delta_{\alpha\alpha'} = \frac{1}{2}(1 + \sigma\sigma')$, $\delta_{\beta\beta'} = \frac{1}{2}(1 + \tau\tau')$ where σ, $\tau = \pm 1$, the (N_α, N_β) model yields the Ising-spin representation of the Ashkin-Teller model,[4,34]

$$\frac{\mathcal{H}}{k_B T} = -\sum_{\langle i,j \rangle} (K_\sigma \sigma_i \sigma_j + K_\tau \tau_i \tau_j + \Lambda \sigma_i \tau_i \sigma_j \tau_j + C) \quad . \tag{3.25}$$

The coupling constants K_σ, K_τ, Λ are related to the variables (3.3) by

$$x_\sigma = \exp[-2(K_\sigma + \Lambda)]; \quad x_\tau = \exp[-2(K_\tau + \Lambda)];$$
$$z = \exp[-2(K_\sigma + K_\tau)] \quad . \tag{3.26}$$

The model is invariant under all permutations of $(K_\sigma, K_\tau, \Lambda)$. On the plane $x_\sigma = x_\tau$, the model can be interpreted as an XY model with fourfold anisotropy[15] of infinite strength. When $x_\sigma = x_\tau$, the nearest-neighbor energies of the Ashkin-Teller model separate into three classes with 1, 2, 1 states of energy K_{00}, $K_{10} = K_{10}$, and K_{11}, respectively. Equivalently, the model can be expressed in terms of two-component vectors at each lattice site pointing into the four directions $(\pm 1, 0)$, $(0, \pm 1)$ and the nearest-neighbor interaction energies

$$-E(\phi = 0)/k_B T = 2K + \Lambda + C = K_{0,0} \quad ,$$
$$-E(\phi = 90\,^\circ)/k_B T = -\Lambda + C = K_{0,1} = K_{1,0} \quad , \tag{3.27}$$
$$-E(\phi = 180\,^\circ)/k_B T = -2K + \Lambda + C = K_{1,1} \quad .$$

In Sec. IV B, we will return to the discussion of the symmetries of the Ashkin-Teller model.

d. *Six-state planar model.* With $N_\alpha = 3$, $N_\beta = 2$ and general $K_{i,j}$, the nearest-neighbor interaction energies separate into four classes with 1, 2, 2, 1 states, with energies $K_{0,0}$, $K_{1,1}$, $K_{1,0}$, $K_{0,1}$ respectively. The states in this model can be represented in terms of a planar vector that can point in six equivalent directions.[8,9] The relative angle between two nearest neighbors can take the values $\phi = 0$, $60\,^\circ$, $120\,^\circ$, $180\,^\circ$; the respective energies associated with these angles are listed above. The planar vector model with scalar product interactions $E(\vec{S}_1, \vec{S}_2) = A - J\vec{S}_1 \cdot \vec{S}_2$ corresponds to a line in the general (x_α, x_β, z) space, defined by $x_\alpha = z^3$, $x_\beta = z^4$.

e. *Eight-state cubic model.* For the model with $N_\alpha = 4$, $N_\beta = 2$ the nearest-neighbor interaction energies separate into four classes, with 1, 3, 3, 1 states in each. The eight states of this model can be represented by a three-component vector that can point along the diagonals of a cube. The case of scalar product interaction corresponds to the line $x_\alpha = z^2$, $x_\beta = z^3$; in this case the Hamiltonian is equivalent to three decoupled Ising models.

IV. SYMMETRY ANALYSIS OF (N_α, N_β) MODELS

In this section, we determine the symmetry properties of discrete models by deriving by a Hubbard transformation[18] the corresponding continuous-spin LGW Hamiltonians. Specifically, the (2,2), i.e., Ashkin-Teller model, with $x_\sigma = x_\tau$ and the (3,2) model with $x_\alpha = z$ are investigated. Based on the LGW Hamiltonians, the forms of the phase diagrams that can be expected are discussed. The phase transitions are characterized in terms of the different representations of the symmetry groups of the models; various types of multicritical behavior are found. The question arises whether the universality classes of *two*-dimensional models can be determined by the leading terms of LGW expansions. The calculations presented in Sec. V confirm the validity of the expectations based on the symmetry analysis.

A. Hubbard transformation

Consider the model with nearest-neighbor coupling,

$$\frac{\mathcal{H}}{k_B T} = -K \sum_{\langle i,j \rangle} \zeta_i \zeta_j = -\tfrac{1}{2} K \tilde{\zeta} A \zeta \quad , \tag{4.1}$$

defined in terms of a set of discrete variables ζ_i associated with the sites i of a lattice or, equivalently, in terms of the N_L-component vector ζ (N_L denotes the number of lattice sites) and the matrix A with components $A_{ij} = 1$, when i, j are nearest neighbors, and $A_{ij} = 0$, otherwise. Using the identity

$$\exp(\tfrac{1}{2} K \tilde{\zeta} A \zeta) = C \int_{-\infty}^{+\infty} \prod_i dS_i \times \exp(-\frac{1}{2K} \tilde{S} A^{-1} S + \tilde{S} \zeta) \quad , \tag{4.2}$$

with $C = (\det A)^{-1/2}$ and a continuous variable S_i associated with each site i, the partition function for

this model is expressed as[18]

$$Z=\sum_{\{\zeta\}}\exp\left(\tfrac{1}{2}K\,\tilde{\zeta}\,A\,\zeta\right)$$
$$=C\int_{-\infty}^{+\infty}\prod_i dS_i\exp\left[-\frac{1}{2K}\,\tilde{S}\,A^{-1}S-\sum_i g(S_i)\right]\ , \tag{4.3}$$

where

$$\exp[-g(S)]=\sum_{\zeta}e^{\tilde{S}\,\zeta}\ . \tag{4.4}$$

The coupling between sites is contained in the first term in the exponential; expansion of $g(S)$ into powers of S yields the appropriate local anisotropy terms. The procedure is easily generalized to models where more than one discrete variable is associated with each lattice site.

B. Ashkin-Teller model

The Ising-spin representation of the Ashkin-Teller model is given by Eq. (3.25). Here the model with the special symmetry $x_\sigma=x_\tau$ is considered. By introducing three continuous variables $S_i^{(k)}$, $k=1,2,3$, for each site i, the partition function can be written

$$Z=C\int_{-\infty}^{+\infty}\prod_i dS_i^{(1)}\,dS_i^{(2)}\,dS_i^{(3)}\exp\left[-\frac{1}{2K}\left(\tilde{S}^{(1)}A^{-1}S^{(1)}+\tilde{S}^{(2)}A^{-1}S^{(2)}\right)-\frac{1}{2\Lambda}\,\tilde{S}^{(3)}A^{-1}S^{(3)}-\sum_i g(S_i^{(1)},S_i^{(2)},S_i^{(3)})\right]\ , \tag{4.5}$$

with

$$g(S^{(1)},S^{(2)},S^{(3)})=-\ln\sum_{\sigma,\tau=\pm1}\exp(\sigma S^{(1)}+\tau S^{(2)}+\sigma\tau S^{(3)})\ . \tag{4.6}$$

Expanding g in powers of $S^{(k)}$ yields

$$g(S^{(1)},S^{(2)},S^{(3)})=-\ln 4-\tfrac{1}{2}\sum_k S^{(k)2}-S^{(1)}S^{(2)}S^{(3)}+\tfrac{1}{12}\sum_k S^{(k)4}+O(S^{(k)6})\ . \tag{4.7}$$

What is the phase diagram of the model in the (K,Λ) plane? Consider first the *quadratic* terms in Eqs. (4.5) – (4.7). Up to this order, the Hamiltonian is identical to that of a magnetic system with tetragonal symmetry. When $K>>\Lambda$, one expects XY type ordering in the "easy plane" $(S^{(1)},S^{(2)})$, while, when $K<<\Lambda$, one expects the $S^{(3)}$ component to undergo an Ising type transition.[35] In the absence of the coupling term of third order, $S^{(1)}S^{(2)}S^{(3)}$, these two lines would meet at a multicritical point of Heisenberg character on the $K=\Lambda$ line. However, the third-order coupling term changes the Hamiltonian at this point to that of the four-state Potts model.[33]

For $K>>\Lambda$ the $S^{(3)}$ component is not critical and can be eliminated by integration, treating the coupling term in perturbation theory. This yields a reduced Hamiltonian that depends on $S^{(1)}$ and $S^{(2)}$ with a coupling term of the form $\sim\Lambda(S^{(1)}S^{(2)})^2+O(S^6)$. Thus the reduced Hamiltonian is that of an XY model with fourfold (or "cubic") anisotropy. Previous studies of such a model indicate the existence of a marginal operator, and continuously varying exponents.[8,15] Since our treatment shows a continuous variation of the anisotropy with Λ, a continuous variation of the exponents along the line of XY type transitions is expected for the Ashkin-Teller model in the $K>\Lambda$ regime.[36] One notes also that the sign of the fourth-order anisotropy is such that $\langle S^{(1)}S^{(2)}\rangle\neq0$ in the ordered phase. Thus as the $S^{(1)}$, $S^{(2)}$ components order, they induce via the third-order coupling term an effective ordering field on $S^{(3)}$, so that no further transitions associated with this field are expected in the ordered phase.

In the regime $K<\Lambda$, the situation is different. Then one expects an Ising-like transition into a phase with $\langle S^{(3)}\rangle\neq0$. Replacing $S^{(3)}$ in Eq. (4.6) by $\langle S^{(3)}\rangle$,

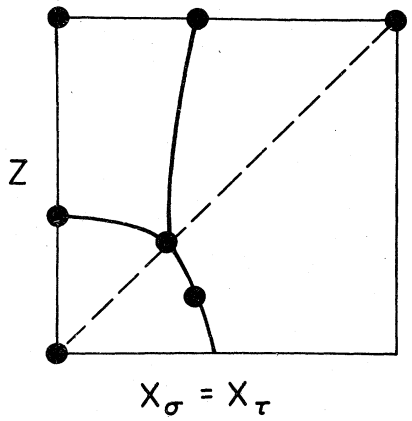

FIG. 5. Schematic phase diagram for the Ashkin-Teller model with $x_\sigma=x_\tau$. The coupling parameters are defined by Eq. (3.26). The system undergoes either one or two transitions, depending on the relative magnitude of the coupling constants. The transition at $x_\sigma=x_\tau=z$ is in the class of the four-state Potts model. The heavy dots represent fixed points of a renormalization-group transformation and are explained in Sec. V E.

a reduced Hamiltonian of the form

$$r[(S^{(1)})^2+(S^{(2)})^2]+w\langle S^{(3)}\rangle S^{(1)}S^{(2)}$$
$$+\text{higher-order terms}$$

is obtained. Upon performing a 45° rotation in the $(S^{(1)},S^{(2)})$ plane, it becomes

$$r[(S^{(+)})^2+(S^{(-)})^2]+\bar{g}[(S^{(+)})^2-(S^{(-)})^2]+\cdots \ .$$

Since $\bar{g}\propto\langle S^{(3)}\rangle$, one of the component ($S^{(+)}$ or $S^{(-)}$, depending on the sign of $\langle S^{(3)}\rangle$) will order for sufficiently large values of $|\langle S^{(3)}\rangle|$, while the other will be noncritical. Thus, when $K<\Lambda$ a second line of Ising transitions is expected to exist in the ordered phase. These considerations lead to the phase diagram of Fig. 5.

Finally, note that the LGW Hamiltonian of Eqs. (4.5) – (4.7) can be viewed as that of a system with the point-group symmetry $4mm$. The two components $(S^{(1)},S^{(2)})$ transform[37] as the two-dimensional irreducible representation E, whereas $S^{(3)}$ belongs to the one-dimensional representation B_2. On the line, $K=\Lambda$, exhibiting the four-state Potts symmetry, the two representations become degenerate; thus the Potts multicritical point is analogous to the more standard case of bicritical points.[35]

C. Cubic model

As discussed in Sec. III C, the (3,2) model on the $x_\alpha=z$ plane possesses cubic symmetry. In order to demonstrate this point in terms of a continuous-spin LGW Hamiltonian, we first rewrite Eq. (3.24) in terms of new variables. The six states associated with each site can be represented by means of a three-component vector $\vec{S}_i=(S_i^{(1)},S_i^{(2)},S_i^{(3)})$ that assumes the values $(\pm1,0,0)$; $(0,\pm1,0)$; $(0,0,\pm1)$. In terms of these variables the Hamiltonian (3.24) takes the form (for $x_\alpha=z$)

$$\frac{\mathcal{H}}{k_BT}=-\sum_{\langle i,j\rangle}[K\vec{S}_i\cdot\vec{S}_j+J(Q_i^{(1)}Q_j^{(1)}+Q_i^{(2)}Q_j^{(2)})] \ , \tag{4.8}$$

where

$$Q^{(1)}=2^{-1/2}[(S^{(1)})^2-(S^{(2)})^2] \ ,$$
$$Q^{(2)}=(\tfrac{2}{3})^{-1/2}[(S^{(3)})^2-\tfrac{1}{3}|\vec{S}|^2] \ . \tag{4.9}$$

The correspondence between K and J and the relative angles between spins is: $E(90°)=-J/3$ and $E(180°)=-K+2J/3$. To perform the Hubbard transformation, we introduce for each site five fields: ϕ_α, $\alpha=1,2,3$ and ψ_β, $\beta=1,2$. The partition function can be expressed in terms of ϕ_α and ψ_β as

$$Z=\int_{-\infty}^{\infty}\prod_{i,\alpha,\beta}d\phi_{\alpha,i}\,d\psi_{\beta,i}\exp\left[-\frac{1}{2K}\sum_\alpha\tilde{\phi}_\alpha A^{-1}\phi_\alpha-\frac{1}{2J}\sum_\beta\tilde{\psi}_\beta A^{-1}\psi_\beta-\sum_i g(\phi_{\alpha,i},\psi_{\beta,i})\right] \ , \tag{4.10}$$

where

$$g(\phi_\alpha,\psi_\beta)=-\ln 6-\frac{1}{6}\left\{\left[\sum\phi_\alpha^2+\sum\psi_\beta^2\right]+54^{-1/2}\ (\psi_2^3-3\psi_1^2\psi_2)+2^{-1/2}\left[\psi_1(\phi_1^2-\phi_2^2)+3^{-1/2}\psi_2\left[3\phi_3^2-\sum_\alpha\phi_\alpha^2\right]\right]\right.$$
$$\left.+\frac{1}{12}\left[\sum_\alpha\phi_\alpha^4-\left[\sum_\alpha\phi_\alpha^2\right]^2\right]\right\}+O(\phi^6,\phi^2\psi^2,\psi^4) \ . \tag{4.11}$$

The symmetry and expected phase diagram of this model can be analyzed in a manner similar to that used for the Ashkin-Teller model. The fields ϕ_α transform like the three-dimensional representation T_1 of the cubic group,[37] while the ψ_β span the two-dimensional representation E. At $K=J$, the two representations are degenerate and the system has the symmetry of the six-state Potts model. For $K>>J$, the ψ fields can be integrated out leaving a reduced Hamiltonian that will exhibit a transition in the universality class of a Heisenberg system with cubic anisotropy. Again, ordering of the ϕ fields induces an ordering field on ψ, so that in this regime the transition takes the system to a phase with both $\langle\phi\rangle\neq0$ and $\langle\psi\rangle\neq0$. In the regime $K<<J$, ordering of the ψ fields [which have the symmetry of the three-state Potts model, as seen by Eq. (4.11)] does not produce an ordering field on ϕ, but rather singles out one ϕ component, lowers its quadratic coefficient, and leads to an Ising-like transition within the partially ordered ($\langle\psi\rangle\neq0$) phase. Thus, on grounds of these considerations one expects a phase diagram as shown in Fig. 6. At the "multicritical" six-state Potts point the transition is first order.[29] Therefore, one may expect (two or three) first-order transition lines to extend from the Potts point and new tricritical points that separate them from the second-order lines.

Finally, we note that the duality transformation discussed in Sec. III B maps the cubic model onto the $x_\beta=z$ plane of the (3,2) model. Repeating an analysis along similar lines as above, yields for this model a LGW Hamiltonian that is *not* identical with Eqs. (4.10) and (4.11). Thus two Hamiltonians of

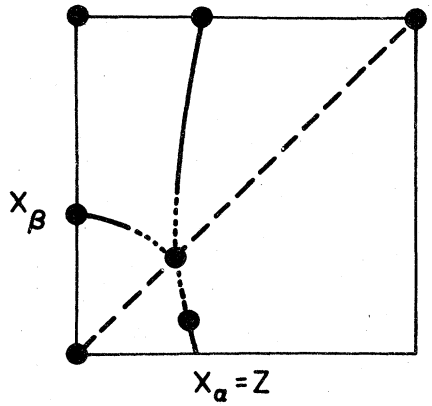

FIG. 6. Schematic phase diagram for the $N_\alpha = 3$, $N_\beta = 2$ model on the cubic plane $x_\alpha = z$. The coupling parameters are defined by Eq. (3.3). The system undergoes either one or two transitions depending on the relative magnitude of the coupling constants. The different phases (I–III) are defined as in Fig. 4. The transition at $x_\alpha = x_\beta = z$ is in the class of the six-state Potts model and is expected to be of first order. The precise character of the phase diagram in the vicinity of this point, P, is unknown. The heavy dots represent fixed points of a renormalization-group transformation and are explained in Sec. V F.

different symmetry are expected to yield the same critical behavior since the original systems are related by a duality transformation.

V. MIGDAL RECURSION RELATIONS FOR THE (N_α, N_β) MODEL

Migdal proposed a remarkably simple method for obtaining approximate recursion relations for complicated systems.[16] The Migdal method[16,23] offers itself for a first, approximate investigation of the (N_α, N_β) model since duality relations exist for the latter.

A. Hamiltonian flow and phase diagrams

Determining the phase diagram for a specific (N_α, N_β) model amounts to finding in the physical region of coupling parameters, $0 \leq x_\alpha, x_\beta, z \leq 1$, the surfaces that separate different phases. This information can be obtained by studying the Hamiltonian flows generated by renormalization-group recursion relations. In order to obtain a phase diagram that is consistent with the exact results summarized in Fig. 3, it is essential to define a renormalization-group transformation that preserves all symmetries of the model. An attempt to formulate recursion relations for the (N_α, N_β) model based on the Niemeijer–van Leeuwen method[21] was unsuccessful in that respect. A formulation based on Migdal's scheme proved successful and is described here. The approximate Migdal recursion relations for the (N_α, N_β) model yield phase diagrams in agreement with all exact results, except questions related to the first-order nature of the $N > 4$ Potts transition. The latter question has not yet been resolved by any of the approximate position space renormalization-group methods.[38]

B. Migdal recursion relations

The Migdal method uses a bond-shifting and decimation procedure to generate recursion relations, as shown schematically in Fig. 1.[23] First, n vertical bonds are shifted. This leaves horizontal chains of n sites that connect sites with $(n+1)$-fold vertical bonds. Second, the trace over the degrees of freedom associated with the n internal sites of each chain is performed. This yields horizontal effective couplings between the vertically coupled sites. Finally, by shifting n of these effective coupling, the new horizontal bonds are defined. Now the vertical chains of n sites are contracted, which defines the new vertical bonds. It is sufficient to follow the renormalization of the horizontal bonds.

For a complicated model, such as the (N_α, N_β) model of Eq. (3.2), carrying out the decimations is the crucial step in Migdal's procedure. It amounts to raising the transfer matrix U of the system [see Eqs. (3.14) and (3.15)] to the power $\lambda = n+1$. This is conveniently done by first diagonalizing U and then raising its eigenvalues to the λ power. According to Eq. (3.17), the eigenvalues of U are $e^{\tilde{K}}$, where $\tilde{K}$ denotes the dual couplings. Thus the decimation yields an effective interaction whose dual is $e^{\lambda\tilde{K}}$. A duality transformation on these yields the "direct" effective couplings, $e^{\hat{K}}$. The last step of adding λ of these effective couplings produces the final result in the form $e^{K'} = e^{\lambda\hat{K}}$. In terms of the variables $\vec{x}$ and functions $\vec{D}$ defined by Eqs. (3.3) and (3.18), the Migdal transformation for the (N_α, N_β) model assumes the form

$$\vec{x}' = \vec{D}^{\lambda}[\vec{D}^{\lambda}(\vec{x})] \ . \tag{5.1}$$

Note that $\vec{D}(\vec{x})$ gives the dual couplings $\tilde{\vec{x}}$, which are then raised to the power λ; a duality transformation on $\vec{D}^{\lambda}(\vec{x})$ gives the direct effective couplings (after the decimation), which then are raised to the power λ. Equations (5.1) define approximate recursion relations that generate the renormalization-group flow in the space of coupling parameters (x_α, x_β, z). The critical points of the (N_α, N_β) models are given by the fixed points of the recursion relations. In analogy to Kadanoff's result,[23] one expects that the equations yield the exact values for all Potts-like transition temperatures in the limit $\lambda \to 1$.

C. Conservation of symmetries

The recursion relations (5.1) preserve the symmetries and special cases of the (N_α,N_β) model discussed in Sec. III.

In the case $x_\alpha x_\beta = z$, which corresponds to that of two decoupled, N_α-component and N_β-component Potts systems, Eq. (3.20) implies

$$\tilde{x}_\alpha = D_\alpha(x_\alpha,x_\beta,x_\alpha x_\beta) = D_{\alpha,p}(x_\alpha) \ , \tag{5.2}$$

where $D_{\alpha,p}$ denotes the duality transformation for an N_α-component Potts system. A similar relation holds for $\tilde{x}_\beta$ and, of course, $\tilde{z} = \tilde{x}_\alpha \tilde{x}_\beta$. Using these results in Eq. (5.1) one obtains

$$\begin{aligned} x_\alpha' &= D_\alpha^\lambda [D_{\alpha,p}^\lambda(x_\alpha), D_{\beta,p}^\lambda(x_\beta) \ , \ D_{\alpha,p}^\lambda(x_\alpha) D_{\beta,p}^\lambda(x_\beta)] \\ &= D_{\alpha,p}^\lambda [D_{\alpha,p}^\lambda(x_\alpha)] \ , \\ x_\beta' &= D_{\beta,p}^\lambda [D_{\beta,p}^\lambda(x_\beta)] \ , \\ z' &= x_\alpha' x_\beta' \ . \end{aligned} \tag{5.3}$$

Thus the decoupled surface is invariant under the Migdal transformation, and the fixed-point structure on this surface is that of Fig. 3.

When $x_\alpha = x_\beta = z$, the (N_α,N_β) model assumes the symmetry of an $N_\alpha N_\beta$-component Potts model. Equation (3.21) implies

$$D_\alpha(\vec{x}) = D_\beta(\vec{x}) = D_z(\vec{x}) = D_{\alpha\beta,p}(z) \ , \tag{5.4}$$

which yields $x_\alpha' = x_\beta' = z'$; therefore, the transformation has a fixed point which corresponds to the $N_\alpha N_\beta$-component Potts model transition.

In the cases when either $x_\alpha = z$ or $x_\beta = z$, the (N_α,N_β) model can be viewed as a discrete spin model with two special symmetries. [See Sec. III C (b).] The Migdal transformation preserves these symmetries. According to Eq. (3.18), $x_\alpha = z$ and $x_\beta = z$ imply $\tilde{x}_\beta = \tilde{z}$ and $\tilde{x}_\alpha = \tilde{z}$, respectively. Therefore, when $x_\alpha = z$ then

$$\begin{aligned} x_\alpha' &= D_\alpha^\lambda(\tilde{x}_\alpha^\lambda, \tilde{z}^\lambda, \tilde{z}^\lambda) \\ &= D_z^\lambda(\tilde{x}_\alpha^\lambda, \tilde{z}^\lambda, \tilde{z}^\lambda) = z' \ , \end{aligned} \tag{5.5}$$

and, similarly, when $x_\beta = z$ then $x_\beta' = z'$. Thus the two planes $x_\alpha = z$ and $x_\beta = z$ are invariant under the transformation (5.1). As exhibited in Fig. 3, the intersection of the decoupled surface, $x_\alpha x_\beta = z$, and the plane $x_\alpha = z$ contains the line $x_\alpha = z = 0$ and also the line $x_\beta = 1$, $x_\alpha = z$. Hence the $x_\alpha = z$ plane contains five of the fixed points exhibited in Fig. 3. The $N_\alpha N_\beta$ Potts fixed point is on the $x_\alpha = z$ plane, too. Similar statements hold for the $x_\beta = z$ plane.

D. Recursion relations in the limit $\lambda \to 1$

The rescaling parameter λ in the recursion relations (5.1) can be analytically continued to $\lambda = 1$. Some properties of the resulting differential recursion relations are discussed below.

For simplicity consider first the recursion relations for the N-component Potts model,

$$x' = D^\lambda[D^\lambda(x)] \ , \tag{5.6}$$

with

$$D(x) = (1-x)/[1+(N-1)x] \ . \tag{5.7}$$

By substituting into Eq. (5.6) $\lambda = 1+\delta$, expanding in δ, and taking the limit $\delta \to 0$, one obtains the differential recursion relation

$$\frac{dx}{dl} = x \ln x + \bar{D}(x) D(x) \ln D(x) \ , \tag{5.8a}$$

where

$$\begin{aligned} \bar{D}(x) &= \left[\frac{dD(y)}{dy} \right]_{y=D(x)} \\ &= -N^{-1}[1+(N-1)x]^2 \ . \end{aligned} \tag{5.8b}$$

Kadanoff[23] found that the Potts transition point,

$$x_p^* = (1+N^{1/2})^{-1} \ , \tag{5.9}$$

is a fixed point of Eq. (5.8a). A self-dual point, x^*, is a fixed point of Eq. (5.8a) only if it satisfies also

$$D(x^*) = -1 \ . \tag{5.10}$$

Linearizing Eq. (5.8a) about the fixed point (5.9) yields the thermal eigenvalue

$$\lambda_T = 2[1 - N^{-1/2} \ln(1+N^{1/2})] \ . \tag{5.11}$$

The recursion relation (5.8a) exhibits a critical fixed point for all values of N, in contradiction to an exact result by Baxter[29] according to which the transition of the two-dimensional Potts model is first order when $N \geq 5$. The failure to produce this exact result is shared by all approximate position space renormalization-group methods.[38]

For the (N_α,N_β) model, the differential recursion relations are

$$\frac{dx_i}{dl} = x_i \ln x_i + \sum_j \bar{D}_{i,j} D_j(x) \ln D_j(\vec{x}) \ , \tag{5.12a}$$

$i,j = 1,2,3$, where the functions D_j are defined by Eq. (3.17), and

$$\bar{D}_{i,j} = \left[\frac{\partial D_i(\vec{y})}{\partial y_j} \right]_{\vec{y}=\vec{D}(\vec{x})} \ . \tag{5.12b}$$

These differential equations exhibit the same fixed-

point structure as the discrete recursion relations. However, they also preserve the self-duality symmetry. A self-dual point $\vec{x}^*$ is a fixed point only if it satisfies also the condition

$$\det(\delta_{ij}+\bar{D}_{ij})=0 \ . \tag{5.13}$$

The results in Sec. V E are based on the differential recursion relations (5.12); those in Sec. V F were obtained numerically using the discrete recursion relations (5.1) with $\lambda=2$.

E. Phase diagram for the Ashkin-Teller model

The approximate Migdal recursion relations (5.12) reproduce the phase diagram proposed by Wu and Lin[39] for the Ashkin-Teller model. As shown in Fig. 7, the phase diagram exhibits five phases and contains fifteen fixed points. The low-temperature fixed point L and the high-temperature fixed point H are completely stable and their three-dimensional domains of attraction constitute fully ordered and disordered phases, respectively. There are three more completely stable fixed points, L_k, at (1,0,0), (0,1,0), and (0,0,1). the domain of attraction of each of these corresponds to an α (or β) ordered and β (or α) disordered phase. These five three-dimensional phases are separated by two-dimensional surfaces. These surfaces are the domains of attraction of singly unstable fixed points. Three of these surfaces constitute the boundaries of the ordered phase, i.e., of the domain of attraction of L. The renormalization-group trajectories originating on these three surfaces flow into one of the three fixed points J_k at $(u^*,0,0)$, $(0,u^*,0)$ or $(0,0,u^*)$, where $u^*=1/(1+2^{1/2})$. The other three surfaces bound the fully disordered phase, and are the domains of attraction of the fixed points I_k at $(u^*,u^*,1)$, $(u^*,1,u^*)$, or $(1,u^*,u^*)$. The two-dimensional surfaces join along three lines. On each line lies one of a set of three doubly unstable fixed points D_k, which is the sink for the flow *along* the line. The coordinates of the fixed points D_k are (u^*,u^*,u^{*2}), (u^*,u^{*2},u^*), and (u^{*2},u^*,u^*). The three lines meet at a completely unstable fixed point, P, located at (v^*,v^*,v^*), where $v^*=(1+4^{1/2})$. At the fixed point P the model has the symmetry of a four-state Potts model. For the physical interpretation of the other fixed points, note that each one of them lies on at least one decoupled surface (as discussed in Sec. III A, there are three such surfaces, namely $x_\sigma x_\tau=z$ and its permutations). For example, the $x_\sigma x_\tau=z$ surface [corresponding to $\Lambda=0$ in Eqs. (3.25) and (3.26)] contains L and H, where both the σ and τ variables are at $T=0$ and $T=\infty$, respectively; at L_1 the σ system is at $T=\infty$ while the τ system is at $T=0$, and at L_2 vice versa. At the two points J_1, J_2 one system is critical while the other is at $T=0$; at I_1, I_2 one is critical and the other at $T=\infty$. At D_1 both systems are critical, i.e., D_1 is a decoupled multicritical point. J_k, I_k, and D_k are Ising fixed points; thus on all surfaces and lines the Migdal approximation yields Ising-like behavior. However, since the Ashkin-Teller model maps onto a staggered eight-vertex model,[32] nonuniversal behavior is expected to occur on the lines that contain D_k. Such behavior would manifest itself in the existence of a marginal operator along these lines. The approximation does not yield this result. Finally, the phase diagram in the $x_\sigma=x_\tau$ plane (i.e., for $K_\sigma=K_\tau$), is given in Fig. 5. As discussed in Sec. III C, on this plane the system exhibits the symmetry of an XY model with fourfold anisotropy. However, depending on the relative magnitude of z vs $x_\sigma=x_\tau$, the critical behavior is either one transition with continuously varying exponents, or of the four-state Potts type, or two Ising transitions. The discussion in Sec. IV B had yielded these results based on symmetry arguments.

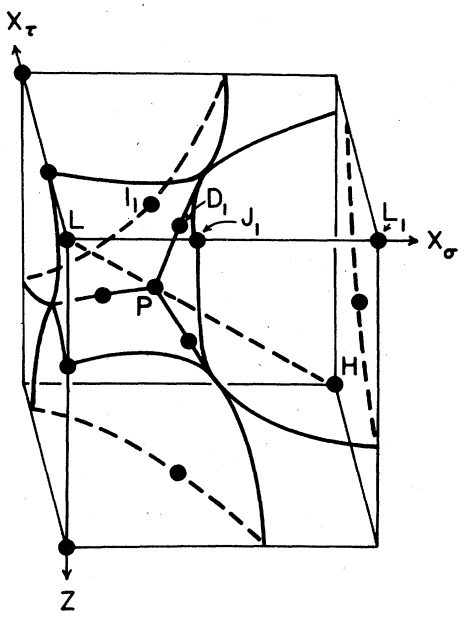

FIG. 7. Phase diagram of the Ashkin-Teller model for general x_σ, x_τ, z. A completely ordered and a completely disordered phase are separated by three distinct partially ordered phases. The latter are bound by surfaces of Ising-like transitions. These surfaces meet at lines on which nonuniversal critical behavior is expected. The approximate Migdal renormalization-group method yields no marginal operator and the Ising-like fixed points on these lines are stable. The three lines meet at a fixed point P of four-state Potts character.

F. Phase diagram for the (3,2) model

The phase diagram of the (N_α, N_β) model with $N_\alpha = 3$, $N_\beta = 2$ is shown on Fig. 8. There are four completely stable fixed points, whose domains of stability constitute four phases. The low-temperature and high-temperature fixed points L and H are associated with the completely ordered and completely disordered phases. The fixed point L_α governs the domain in which the α system is ordered while the Ising-like β system is disordered, and vice versa for L_β. The four phases are separated by five two-dimensional surfaces. These surfaces are the domains of attraction of five singly unstable fixed points. Four of these, J_1, J_2 and I_1, I_2 lie on the decoupled surface $x_\alpha x_\beta = z$. At I_1 and I_2 the β system is critical while the α system is in the state $T=0$ and $T=\infty$, respectively, whereas at J_1 and J_2 the three-state Potts α system is critical and the β system is at $T=0$ or $T=\infty$, respectively. Thus on the four surfaces that flow into I_k and J_k, $k=1,2$, either Ising or three-state Potts critical behavior is expected. The four surfaces meet on a segment of the self-dual line defined by

$$1+2x_\alpha+x_\beta+2z=6^{1/2}\ ,$$
$$x_\alpha+x_\beta+(6^{1/2}-1)z=1\ ,$$
$$z<(1+6^{1/2})^{-1}\ . \tag{5.14}$$

This line is the domain of attraction of the doubly unstable decoupled multicritical fixed point D. No marginal operator is expected on this line, since Kadanoff and Wegner's[36] criterion for nonuniversal behavior is not satisfied for the (3,2) model. The fifth surface in Fig. 8 separates the completely ordered and completely disordered phases. This surface is the domain of attraction of the self-dual fixed point S. The surface merges with two other surfaces along a line that lies in the $x_\alpha = z$ plane, and along a line in the $x_\beta = z$ plane. Each of these lines is the domain of attraction of a fixed point. The fixed point C on the line in the $x_\alpha = z$ plane describes cubic critical behavior. The fixed point $\tilde{C}$, on the line in the $x_\beta = z$ plane is the dual of C. These two lines and the self-dual line meet at the completely unstable six-state Potts fixed point, P.

For any specific system, varying the temperature defines a line $\bar{L}(T)$ in the (x_α, x_β, z) space. The line connects the points (0,0,0) and (1,1,1) in Fig. 8 and, in general, will cross either two or one critical surface(s). When two surfaces are crossed, the system will undergo an Ising plus a three-state Potts transition, even though the two types of variables are coupled in the (3,2) model. In the special case when the trajectory crosses the segment of the self-dual line defined by Eq. (5.14), the Ising and three-state Potts transitions occur at the same temperature and conventional scaling[40] breaks down.

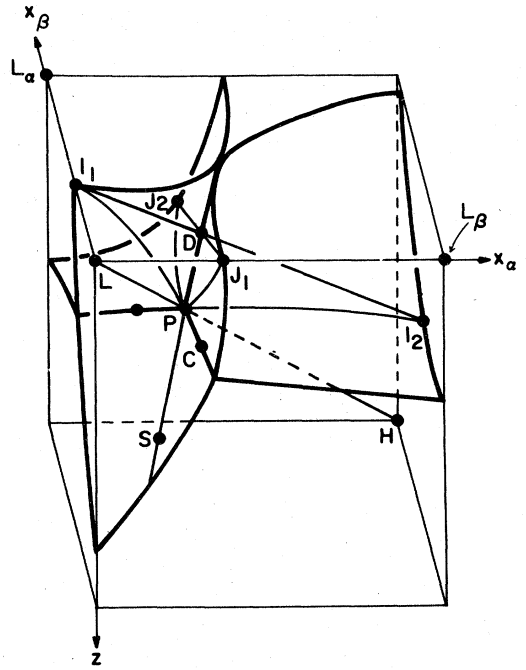

FIG. 8. Phase diagram of the $N_\alpha = 3$, $N_\beta = 2$ model, as obtained by Migdal recursion relations. The fixed points are $L(H)$, low (high) temperatures; D, decoupling Ising and three-state Potts; P, six-state Potts; S, self-dual; C, cubic; I_1, I_2, Ising; J_1, J_2, three-state Potts. The plane $x_\alpha = z$ corresponds to the subspace of cubic symmetry; it contains cubic, Ising, and three-state Potts transition lines that meet at P.

The phase diagram of Fig. 8 contains information about the special cases of the (3,2) model that were discussed in Sec. III. If the parameters of a system satisfy $z > x_\alpha, x_\beta$, at the phase transition point, the system will exhibit a single phase transition with critical behavior determined by the self-dual fixed point S. The six-state planar model of Sec. III C belongs to this category. José *et al.*[8] proposed a phase diagram for an XY system with weak sixth-order anisotropy. They found the anisotropy in a region of temperatures, $T_1 < T < T_2$, to be irrelevant with the renormalization-group trajectories flowing into a segment of the isotropic Berezinskii line.[41] The model discussed here represents the extremely anisotropic limit of the model considered by these authors. Therefore, on the basis of the Migdal approximation presented here, the two lines that bound the domain of stability of the Berezinskii line must join in order to allow for a single transition in the infinite anisotropy limit.

The phase diagram of the model on the cubic plane, $x_\alpha = z$, is shown in Fig. 6. The Migdal calculation yields incorrectly the result that all phase transitions, including the six-state Potts one, are of second order. For $x_\beta < x_\alpha = z$ the system undergoes *one*

TABLE I. Fixed-point coordinates and exponents for the $N_\alpha=3$, $N_\beta=2$ model from Migdal's recursion relations, Eq. (5.1), with $\lambda=2$. For the notation of the fixed points see the text and Fig. 8.

Fixed Point	P	C	S	D
x_α	0.183	0.209	0.055	0.250
x_β	0.183	0.084	0.0065	0.295
z	0.183	0.209	0.469	0.074
y_1	0.97	0.92	0.17	0.75
y_2	0.26	0.50	−1.10	0.83
y_3	0.26	−0.33	−3.58	−0.42

phase transition governed by the cubic fixed point. When $x_\alpha=x_\beta=z$ a six-state Potts transition occurs, and for $x_\beta > x_\alpha=z$ the system undergoes a three-state Potts transition *and* at a lower temperature an Ising-like transition. Again, these results agree with the discussion of the phase diagram by symmetry arguments. On the $x_\beta=z$ plane the system has a different symmetry (see Sec. IV C). However, since the $x_\beta=z$ plane is dual to the $x_\alpha=z$ plane, the critical behavior of these two systems is expected to be identical even though their symmetries are different. The locations of the fixed points and results for the exponents are summarized in Table I.

Finally, for the (4,2) model we expect a phase diagram similar to that of Fig. 8, however, with four-state Potts fixed points and surfaces replacing the three-state Potts ones, and an eight-state Potts point replacing the six-state Potts point. Also, in this case the self-dual fixed point, S, describes three decoupled Ising systems.

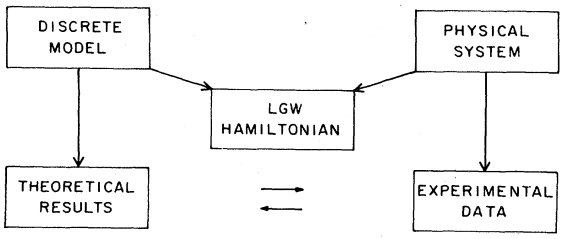

FIG. 9. Procedure by which the relation between two-dimensional discrete models and physical systems is established. The connection is made via a LGW expansion of a continuous-spin Hamiltonian.

VI. PHASE TRANSITIONS IN QUASI-TWO-DIMENSIONAL SYSTEMS

Two-dimensional, discrete models and phase transitions in adsorbed systems are related in a three-step approach. The important assumption is the hypothesis that if a discrete spin model and an experimental system are described by the same LGW Hamiltonian, then all three belong to the same universality class.[17] Similar ideas can be applied to phase transitions in layered magnetic compounds. Here the general ideas are described and then applied to the α-β phase transition in overlayers of molecular oxygen on the basal plane of graphite.[24,25] The transition is shown to be in the universality class of the two-dimensional Heisenberg model with cubic anisotropy.

A. Microscopic models for two-dimensional systems

Implicit in our discussion of phase transformations in overlayers is the assumption that the latter constitute ideal films over distances large compared to the correlation length. There are two general assumptions on which the theoretical approach is based. (i) The characteristics of phase transitions in two dimensions are determined by the dimensionality of the order parameter, by the symmetry of the system, and by the range of the forces. (ii) The LGW Hamiltonian concept can be used to establish the connection between a physical system and an appropriate discrete model. We proceed in three steps as summarized in Fig. 9 and outlined below.

The first step toward the determination of the appropriate model is the symmetry analysis of discrete models in terms of a LGW expansion of the corresponding continuous-spin Hamiltonians, as performed in Sec. IV. The mapping of continuous spin onto discrete models discussed in Sec. II, can be used also to establish the connection between the two types of models. The next step requires the knowledge of or assumptions about the symmetries of the ordered and disordered phases of the physical system under consideration. By using Landau symmetry arguments[12,13] the appropriate LGW Hamiltonian for the system is derived. The third step consists in making contact between the discrete model and the physical system based on the following universality hypothesis. When a discrete model and an experimental system are described by the same LGW Hamiltonian, all three belong to the same universality class. Finally, the discrete model is investigated by methods of statistical mechanics.

In summary, the approach uses a generalized Hubbard transformation and symmetry arguments to establish the relation between discrete and continuous spin models. The universality hypothesis of the third step has to be tested by theory and experiment.

B. Tests of the universality hypothesis

There are a few examples where models and/or physical systems have been studied extensively so that aspects of the universality hypothesis can be tested.

The first example is the order-disorder transition in overlayers of ^{4}He on graphite, at $\frac{1}{3}$ coverage.[42] Alexander[19] has shown that the appropriate LGW Hamiltonian is that of the three-state Potts model, for which the latest series estimates[43] yield $\alpha = 0.42 \pm 0.05$ for the specific-heat exponent. This value is consistent with measurements by Bretz,[44] who found $\alpha \approx 0.36$.

Another example concerns the Baxter-Wu "three-spin" model[45] and the four-state Potts model, which yield to leading order identical LGW Hamiltonians. For the Baxter-Wu model the value for α is exactly $\alpha = \frac{2}{3}$,[45] which is consistent with the series expansion result for the four-state Potts model, $\alpha = 0.64 \pm 0.05$.[46] Various physical realizations of this model have been suggested,[20] but no experimental measurement of α has been performed so far.

Finally we mention four distinct models that lead to the LGW Hamiltonian of the XY model with fourfold anisotroy. These are the Ashkin-Teller model,[4] the Baxter eight-vertex model,[5] the Villain model with fourfold symmetry breaking,[8,15] and the Ising model with competing nearest- and next-nearest-neighbor interactions.[2] All four models are expected to possess a marginal operator, and to exhibit critical behavior characterized by continuously varying exponents. A physical realization of a system with this LGW Hamiltonian may be provided by oxygen chemisorbed on the (110) face of tungsten.[47,17]

C. Magnetic phase transition in O_2 on graphite

Films of between one and two layers of molecular oxygen physisorbed on the basal plane of graphite exhibit a magnetic and a distortive phase transition at about 10–12 K, which is apparently continous.[24,25] The transition will be referred to as the α-β transition. Neutron scattering investigations by McTague and Nielsen[24] have revealed information about the structure of the phases. [See Fig. 10(a).] The α-β transition has also been studied via specific-heat measurements by Vilches and Stoltenberg.[25] In the paramagnetic phase the structure is similar to that of the closest-packed plane of β-O_2. The symmetry group is that of a triangular lattice, $P6mm$. The low-temperature phase has a distorted triangular structure analogous to that of the closest-packed plane of bulk α-O_2. This phase exhibits antiferromagnetic order. All data are consistent with the assumption that the O_2 molecular axes are normal to and the magnetic moments confined to the plane of the substrate. The α and β phases are strongly incommensurate with the substrate lattice. Hence, for the theoretical analysis we assume that all substrate effects can be neglected. Bak[48] showed that since the substrate potential has the same symmetry, $P6mm$, as the overlayer in the high-temperature phase, a possible modulation of the latter does not change the conclusions concerning the universality class of the phase transition.

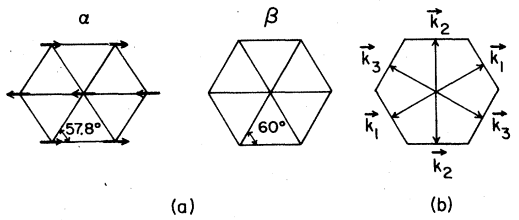

FIG. 10. (a) Structure of the ordered (α) and disordered (β) phases of molecular oxygen adsorbed on graphite. The arrows denote the spin orientations on the distorted triangular lattice. (b) The Brillouin zone and wave vectors, $\vec{k}$, that define the different ordered states.

A LGW Hamiltonian for the α-β transition of O_2 on graphite was proposed[17] that contains the effects of both the magnetic and distortive degrees of freedom.

Consider first the spin degrees of freedom. The spin structure of the ordered state shown in Fig. 10(a) yields a nonvanishing value of the (three component) order parameter

$$\phi_j = \sum_{\vec{R}} \exp(i\vec{k}_j \cdot \vec{R})\, \vec{v}_j \cdot \vec{S}(\vec{R}) \ , \tag{6.1}$$

with the $\vec{k}_j$ shown in Fig. 10(b), and the unit vectors $\vec{v} \perp \vec{k}_j$. The three functions ϕ_j constitute an irreducible representation of the symmetry group $P6mm$ of the high-temperature phase. The magnetic part of the LGW Hamiltonian contains all the invariants that can be constructed from these three functions. Note that time-reversal symmetry [under which $S(\vec{R}) \rightarrow -\vec{S}(R)$] excludes all odd invariants. This leaves, for the magnetic part, the LGW Hamiltonian of a Heisenberg system with cubic anisotropy

$$\mathcal{H}_{\rm mag} = -\left[\tfrac{1}{2} \sum_j (\nabla \phi_j)^2 + \tfrac{1}{2} r_1 \sum_j \phi_j^2 + u\left(\sum_j \phi_j^2 \right)^2 + v \sum_j \phi_j^4 \right] . \tag{6.2}$$

The distortive part of the LGW Hamiltonian depends on the displacements of the O_2 molecules from their positions in the high-temperature phase. Uniform lattice distortions are described in terms of the strain tensor ϵ_{ij}. For a two-dimensional system there are three independent components, ϵ_{xx}, ϵ_{yy},

and ϵ_{xy}. Of these, the combination $\epsilon_{xx}+\epsilon_{yy}$ transforms as the unit representation of $P6mm$, while the two functions

$$\psi_1=\epsilon_{xy},\quad \psi_2=\tfrac{1}{2}(\epsilon_{xx}-\epsilon_{yy}) \tag{6.3}$$

constitute a two dimensional representation. The distortive part of the LGW Hamiltonian, given in terms of invariants up to fourth order, is given by

$$\mathcal{H}_{\text{dist}}=-\left[\tfrac{1}{2}\sum_i(\nabla\psi_i)^2+\tfrac{1}{2}r_2\sum_i\psi_i^2 + w(\psi_2^3-3\psi_1^2\psi_2)+\bar{u}\left(\sum\psi_i^2\right)^2\right] . \tag{6.4}$$

This is exactly the LGW Hamiltonian of the three-state Potts model.

Finally, to identify a term that couples the magnetic and elastic degrees of freedom, we construct an invariant from ϕ_j and ψ_i. The lowest order invariant that can be constructed is quadratic in ϕ_j and linear in ψ_i and is given by

$$\mathcal{H}_{\text{coup}}=(\phi_3^2-\phi_2^2)\psi_1+3^{-1/2}\left(3\phi_1^2-\sum_j\phi_j^2\right)\psi_2 . \tag{6.5}$$

Hence, symmetry arguments yield for the total LGW Hamiltonian describing the α-β transition in O_2 on graphite

$$\mathcal{H}=\mathcal{H}_{\text{mag}}+\mathcal{H}_{\text{dist}}+\mathcal{H}_{\text{coup}} . \tag{6.6}$$

The relative size of the coupling parameters in Eq. (6.6) remains undetermined.

The Hamiltonian (6.6) is identical with the LGW Hamiltonian (4.11) obtained by a Hubbard transformation for the $(N_\alpha=3, N_\beta=2)$ model on the cubic plane $x_\alpha=z$. The phase diagram for this model is exhibited in Fig. 6 and discussed in Secs. IV C and V F. We conclude that depending on the relative size of the coupling parameters r_1 and r_2 in Eqs. (6.2) and (6.4), respectively, the α-β transitions consist of either one or two transitions. The interpretation is as follows. (Compare Sec. IV C for details.) When $r_2 << r_1$, a continuous three-state Potts transition leads to a distorted, but nonmagnetic intermediate phase and then an Ising transition occurs into the low-temperature distorted and antiferromagnetic phase. When $r_2 >> r_1$, a single, continuous phase transition of cubic Heisenberg character into the distorted and magnetic phase occurs. For $r_1=r_2$ the transition is a *first*-order six-state Potts transition. The phase diagram in the vicinity of the point $r_1=r_2$ is not yet understood, and will be more complicated than the approximate Migdal calculation predicts because of the first order nature of the Potts transition. One might expect first-order phase transition lines to extend from $r_1=r_2$ and new tricritical points to separate them from the second-order lines.

The specific-heat[25] and neutron scattering data[24] are consistent with the interpretation that the α-β transition takes place as a single transition. Hence, O_2 on graphite is an excellent candidate for a two-dimensional Heisenberg system with cubic anisotropy. Further studies of the transition and determinations of the critical exponents α and β are needed to confirm that the system belongs to this new universality class. It would also be of interest to study the transition for the system in a magnetic field, $\vec{H}$, applied perpendicular to the substrate. Then

$$\mathcal{H}\rightarrow\mathcal{H}+aH_z^2\vec{\phi}^2+bH_z^2\vec{\psi}^2 , \tag{6.7}$$

with $a>b$. If the system is in the cubic Heisenberg regime, the field is expected to lower the transition temperature. (Mean-field theory yields the estimate $\delta T_c\approx 2$ K per 100 kG.) The intriguing questions are (i) whether the six-state Potts point can be reached with the new first-order multicritical behavior becoming observable and (ii) whether, for sufficiently strong fields, the splitting of the transition into two branches can be found. Application of a field parallel to the substrate should result in two-dimensional *bi*-critical behavior of the usual kind.[35]

VII. SUMMARY

We have investigated two-dimensional anisotropic N-vector models under three viewpoints.

(i) Experimental realizations of two-dimensional anisotropic N-vector models exist. A comprehensive approach to the description of phase transitions in two-dimensional systems was outlined that involves, first, the determination of a model for the system under consideration and, second, the treatment of the model by renormalization group and/or other techniques. The concept of continuous-spin LGW Hamiltonians was used to relate experimental systems and *discrete* models. The universality hypothesis that this reasoning employs, namely, that an experimental system and a discrete model belong to the same universality class when they are described, to leading order, by identical LGW Hamiltonians, has not yet been tested extensively for two dimensions. Examples were given that indicate the validity of the hypothesis.

(ii) Relations among anisotropic continuous-spin Hamiltonians and discrete models were established by Migdal renormalization-group arguments and the Hubbard transformation. Discrete models were conjectured to be equivalent to N-component continuous-spin models with local anisotropies. In two dimensions, symmetry-breaking perturbations of N-vector models with $N\geq 3$ are relevant; in their absence *no* phase transition exists. (For the XY model the fourfold symmetry-breaking term is marginal and leads to the Ashkin-Teller model.) For example, it

was shown that the Migdal recursion relations map the continuous-spin, cubic Heisenberg Hamiltonian onto the discrete cubic model. A verification of this result by a rigorous calculation would be of interest.

(iii) The discrete models with which many of the anisotropic N-vector models are connected have the form of a generalized Potts model. The (N_α, N_β) model was introduced and defined in terms of two coupled Potts-like variables associated with each lattice site and then analyzed by duality and renormalization-group methods. It provides a unified description for large classes of discrete models with nearest-neighbor interactions.

The concepts were exemplified by a discussion of the two-dimensional Heisenberg model with cubic anisotropy, which has applications to the magnetic α-β phase transition in overlayers of oxygen on graphite. Also discussed were new experiments for the study of this system.

ACKNOWLEDGMENTS

We are grateful for the hospitality extended to us by the staff of NORDITA, Copenhagen, especially Dr. Alan Luther, where part of this work was carried out. We acknowledge helpful discussions and/or correspondence with P. Bak, R. B. Griffiths, A. Luther, D. Mukamel, D. R. Nelson, M. Nielsen, O. E. Vilches, and M. Schick, who also commented on the manuscript. One of us (E. D.) acknowledges a Dr. Ch. Weizmann Postdoctoral Fellowship. This work was supported in part by NSF Grant No. DMR77-12676 A01.

[1]N. D. Mermin and H. Wagner, Phys. Rev. Lett. 17, 1133 (1966).

[2]Besides the ordinary Ising model, this includes models with competing nearest- and next-nearest neighbor interactions as discussed, for example, by J. M. J. van Leeuwen, Phys. Rev. Lett. 34, 1056 (1975).

[3]R. B. Potts, Proc. Cambridge Philos. Soc. 48, 106 (1952).

[4]J. Ashkin and E. Teller, Phys. Rev. 64, 178 (1943).

[5]R. J. Baxter, Phys. Rev. Lett. 26, 832 (1971); and Ann. Phys. (N.Y.) 70, 193 (1972).

[6]D. Kim, P. M. Levy, and L. F. Uffer, Phys. Rev. B 12, 989 (1975).

[7]A. Aharony, J. Phys. A 10, 389 (1977).

[8]J. V. José, L. P. Kadanoff, S. Kirkpatrick, and D. R. Nelson, Phys. Rev. B 16, 1217 (1977).

[9]L. Mittag and M. J. Stephen, J. Math. Phys. 12, 441 (1971).

[10]R. A. Pelcovits and D. R. Nelson, Phys. Lett. A 57, 23 (1976).

[11]S. Krinsky and D. Mukamel, Phys. Rev. B 16, 2313 (1977).

[12]L. D. Landau and E. M. Lifshitz, *Statistical Physics* (Addison-Wesley, Reading, Mass., 1969) Chap. XIV.

[13]D. Mukamel and S. Krinsky, Phys. Rev. B 13, 5065 (1976).

[14]M. E. Fisher, Rev. Mod. Phys. 46, 597 (1974); A. Aharony, in *Phase Transitions and Critical Phenomena,* edited by C. Domb and M. S. Green (Academic, London 1976), Vol. 6, p. 357.

[15]Connections between the critical behavior of the XY model with fourfold anisotropy and the eight-vertex and Ashkin-Teller models were discussed by L. P. Kadanoff, Phys. Rev. Lett. 39, 903 (1977); and unpublished.

[16]A. A. Migdal, Zh. Eksp. Teor. Fiz. 69, 1457 (1975) [Sov. Phys. JETP 42, 743 (1976)].

[17]E. Domany and E. K. Riedel, Phys. Rev. Lett. 40, 561 (1978); E. Domany and E. K. Riedel, J. Appl. Phys. 49, 1315 (1978).

[18]G. A. Baker, Phys. Rev. 126, 2071 (1962); J. Hubbard, Phys. Lett. A 39, 365 (1972).

[19]S. Alexander, Phys. Lett. A 54, 353 (1975).

[20]E. Domany, M. Schick, and J. S. Walker, Phys. Rev. Lett. 38, 1148 (1977); E. Domany, M. Schick, J. S. Walker, and R. B. Griffiths, Phys. Rev. B 18, 2209 (1978).

[21]Th. Niemeijer and J. M. J. van Leeuwen, in *Phase Transitions and Critical Phenomena,* edited by C. Domb and M. S. Green (Academic, London 1976), Vol. 6, p. 425.

[22]L. P. Kadanoff, A. Houghton, and M. C. Yalabik, J. Stat. Phys. 14, 171 (1976).

[23]L. P. Kadanoff, Ann. Phys. (N.Y.) 100, 359 (1976).

[24]J. P. McTague and M. Nielsen, Phys. Rev. Lett. 37, 596 (1976); and unpublished.

[25]O. E. Vilches and J. Stoltenberg (unpublished).

[26]S. Gregory, Phys. Rev. Lett. 40, 723 (1978).

[27]C. Jayaprakash, E. K. Riedel, and M. Wortis, Phys. Rev. B 18, 2244 (1978).

[28]A. M. Polyakov, Phys. Lett. B 59, 79 (1975); C. J. Hamer, J. B. Kogut, and L. Susskind, Phys. Rev. Lett. 41, 1337 (1978).

[29]R. J. Baxter, J. Phys. C 6, L445 (1973).

[30]Evidence exists from series data [R. V. Ditzian and J. Oitma, J. Phys. A 7, L61 (1974)], renormalization-group work [G. Golner, Phys. Rev. B 8, 3419 (1973)], and experiments [A. Aharony, K. A. Muller, and W. Berlinger, Phys. Rev. Lett. 38, 33 (1977); B. Barbara, M. F. Rossignol, and P. Bak, J. Phys. C 11, L183 (1978), who use the symmetry analysis by D. Mukamel, M. E. Fisher, and E. Domany, Phys. Rev. Lett. 37, 565 (1976)].

[31]F. Y. Wu and Y. K. Wang, J. Math Phys. 17, 439 (1976).

[32]F. J. Wegner, J. Phys. C 5, L131 (1972).

[33]R. K. P. Zia and D. J. Wallace, J. Phys. A 8, 1495 (1975).

[34]C. Fan, Phys. Lett. A 39, 136 (1972).

[35]J. M. Kosterlitz, D. R. Nelson, and M. E. Fisher, Phys. Rev. B 13, 412 (1976).

[36]L. P. Kadanoff and F. J. Wegner, Phys. Rev. B 4, 3989 (1971).

[37]M. Tinkham, *Group Theory and Quantum Mechanics* (McGraw-Hill, New York, 1964), Appendix B.
[38]See, for example, C. Dasgupta, Phys. Rev. B 15, 3460 (1977).
[39]F. Y. Wu and K. Y. Lin, J. Phys. C 7, L181 (1974).
[40]B. Widom, J. Chem. Phys. 43, 3892 (1965).
[41]V. L. Berezinskii, Zh. Eksp. Teor. Fiz. 59, 907 (1970) [Sov. Phys. JETP 32, 493 (1971)]; Zh. Eksp. Teor. Fiz. 61, 1144 (1971) [Sov. Phys. JETP 34, 610 (1971)].
[42]M. Bretz and J. G. Dash, Phys. Rev. Lett. 27, 647 (1971).
[43]T. de Neef and I. G. Enting, J. Phys. A 10, 801 (1977).
[44]M. Bretz, Phys. Rev. Lett. 38, 501 (1977).
[45]R. J. Baxter and F. Y. Wu, Phys. Rev. Lett. 31, 1294 (1973).
[46]I. G. Enting, J. Phys. A 8, L35 (1975). However, R. Zwanzig and J. D. Ramshaw [J. Phys. A 10, 65 (1977)] found $\alpha = 0.45 \pm 0.02$.
[47]J. C. Buchholtz and M. G. Lagally, Phys Rev. Lett. 35, 442 (1975).
[48]P. Bak (private communication).